Plasma Polymerization of Tetrafluoroethylene in a Field-Free Zone

PETER D. BUZZARD, DAVID S. SOONG, and ALEXIS T. BELL,
Department of Chemical Engineering, University of California, Berkeley, Berkeley, California 94720

Synopsis

Plasma polymerization of tetrafluoroethylene by itself and mixed with inert gases has been studied in the field free zone inside a Faraday cage. The chemical structure was analyzed by ESCA, revealing both linear and branched products. Linear products are formed by less energetic plasmas and at low monomer residence times. Lower energy plasmas result from the use of lower powers and lower percentages of helium in the feed. Production of linear products under these conditions is probably due to lower rates of free radical and metastable formation in the plasma. Through a combination of kinetic and mass transfer effects, shorter monomer residence times under high flow rates and within short distances from the front edge of the electrode give rise to a lower concentration of free radicals at the electrode surface, producing a more linear polymer. Linear products were also formed at very high powers. This latter result is quite unexpected and is probably due to rapid gas phase polymerization. The chemical structure was not affected significantly by the substrate temperature or by hydrodynamics in this work. All of the evidence indicates that the gases were well mixed in the reaction zone for the range of process variables and for the gases studied. The deposition rate was also studied as a function of the reaction conditions. It was affected by the concentration of free radicals, the concentration of the monomer, and the substrate temperature. The observed deposition rate profile across the electrode is consistent with mass transfer and kinetic considerations governing free radical and monomer concentrations on the electrode surface. The deposition rate is greater at the lower substrate temperature used, probably due to enhanced adsorption process.

INTRODUCTION

Polymeric materials can be deposited on a substrate placed in the plasma[1] or glow discharge of an organic vapor. These reaction products are often in a powder form, thin films, oil, or some combination of the above,[2] depending on the reaction conditions and the monomer. The films produced via these processes are typically insoluble, pinhole-free, and adhere well to the substrate. Previous research on hydrocarbon systems has shown that these amorphous films are often highly branched or even crosslinked.[2]

In addition to these plasma products of hydrocarbons, plasma-polymerized fluorocarbons have recently generated considerable interest because of other characteristics. Fluorocarbon polymers produced by conventional bulk polymerization are known to be nonwetting, nonsticking, and highly resistant to chemical attack. Similar behavior is expected of plasma-polymerized fluorocarbons. As a result, plasma polymerized fluorocarbon films have been investigated for several potential uses, such as moisture-resistant protective coatings for alkali metal halide crystals used in laser optics,[3] antireflective coatings for plastic optical lenses,[3,4] corrosion protective coatings for metals,[5] dry lubricant surfaces,[5–7] thin film insulators and capacitors,[8] coatings on fabrics to impart oil and water repellency and soil resistance,[9,10] and metal-containing films for potential electrical, optical, and magnetic applications.[11]

Journal of Applied Polymer Science, Vol. 27, 3965–3985 (1982)
 CCC 0021-8995/82/103965-21$03.10

Several spectroscopic techniques have been used to analyze the gases from and the polymer products of fluorocarbon plasma.[12] Mass spectral studies of gases from a tetrafluoroethylene (TFE) plasma indicate that several neutral species besides the monomer are present, a large number of which are highly unsaturated.[13] Electron spin resonance (ESR) spectroscopy has shown that a high concentration of trapped free radicals exists in fluorocarbon plasma polymers.[14] Electron spectroscopy for chemical analysis (ESCA) has been used[15] to discern the relative abundance of carbon atoms bonded to various numbers of fluorine atoms, e.g., CF_3, CF_2, and CF functional units, along with carbon bonded quaternally to other carbon atoms. Previous ESCA studies concluded that all of these functional groups are present in significant quantities, regardless of the fluorocarbon monomer used.[12,16] Plasma polymerization of fluorocarbons thus involves a high degree of molecular rearrangement.

The effects of radio frequency power, reactor pressure, and monomer flow rate on the deposition rate and the chemical structure of plasma polymerization products have been investigated.[12,16–18] Although a quantitative model of the polymerization kinetics has been presented for hydrocarbon monomers,[19] no such model exists at present for fluorocarbon systems. Yasuda et al.[18,20] reported that the ratio of the radio-frequency power (W) to the monomer flow rate (F) is a relevant parameter in determining the importance of competitive reactions taking place in TFE plasmas. At low values of this parameter, polymerization proceeds primarily via a chain reaction polymerization mechanism ("plasma-induced polymerization"), resulting in products with low levels of molecular rearrangement. At higher values of W/F, reactive intermediates play an increasingly important role in polymer formation, and the products exhibit a greater degree of molecular rearrangement. At still higher values, decomposition of the polymer becomes important, yielding fluorine-poor polymerization products. Nakajima et al.[17] used a similar framework to explain the behavior of the deposition rate in a TFE system.

Polymeric products can also be formed on a substrate placed outside the plasma zone. O'Kane and Rice[5] performed a series of experiments in which a substrate was placed downstream from the plasma zone. Films with a high CF_2 character (95% CF_2 and 5% CF_3 as determined by ESCA) were produced from tetrafluoroethylene. This result indicates that the deposited polymer was mostly linear without significant branching or crosslinking. Pore density tests revealed that, in comparison with crystalline metallic coatings of similar thickness, the polymer formed in the nonglow region provided superior atmospheric protection for transition metal substrates. In addition, these films were insoluble in Freon TF, and had lower surface energies than both Teflon and films formed in the glow discharge. Lower deposition rates were, however, observed in the nonglow region than the glow region. Yasuda et al.[18] also polymerized TFE in a nonglow region and found that polymer with an enhanced CF_2 character was produced under certain conditions.

Polymerization of tetrafluoroethylene inside a Faraday cage has recently been studied.[12,21] A Faraday cage is a metallic screen enclosure. When placed on one of the electrodes of a capacitively coupled system, a field free zone develops within the confines of the cage. As a result, a plasma is generated above the cage but not within it. Using a bell jar reactor, Pender et al.[12] polymerized TFE inside a Faraday cage. Little structural difference was found between the product

formed inside and outside the cage. Salhi[21] carried out further experiments with TFE in a similar system, and found that a product with an enhanced CF_2 character could be produced in the field free zone. Here, the reaction conditions played an important role in determining the chemical structure of the product.

In the present study, the polymerization of tetrafluoroethylene inside a Faraday cage was examined in a tubular flow reactor. Helium and argon were introduced in several experiments in order to investigate the effects of inert gases on the structure of the products and rate of polymerization. The chemical structure, deposition rate, and physical form of the polymerization products deposited in the field free zone were studied as functions of axial position in the reactor, reaction conditions (flow rate and power), substrate temperature, flow pattern of the feed gases through the reactor, and composition of the feed gas.

EXPERIMENTAL

The tubular flow reactor and the associated apparatus are illustrated in Figure 1. The various components of the reactor are housed in a Pyrex cylinder. A rectangular box-shaped Faraday cage is placed on top of the bottom electrode. A plasma or glow discharge is initiated directly above the cage, while a dark or field-free zone is maintained within the cage. The sides of the cage are constructed out of copper sheet metal. The top and ends are made from 16-mesh copper screen. This construction allows both convective flow and diffusion to take place at the top and ends of the cage. Reactive species can thus pass from the plasma zone into the dark zone; however, no reactive species are formed within the dark zone by means of radio frequency excitation. The Faraday cage divides the space between the electrodes into a plasma zone and a dark zone of equal dimensions.

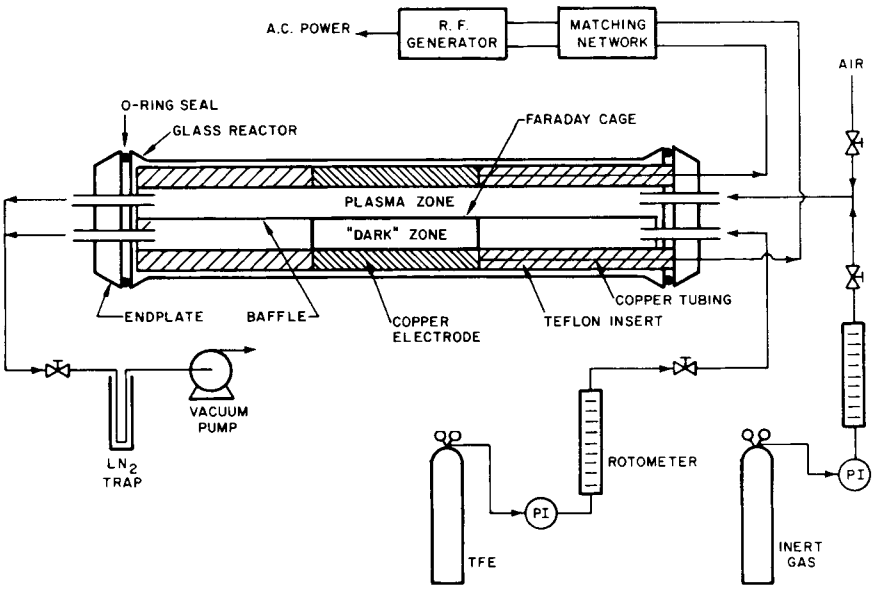

Fig. 1. Plasma polymerization reactor system.

A rectangular Plexiglas box is placed on top of each of the lower Teflon inserts in order to seperate the monomer gas and inert gas. These boxes are open at the ends adjacent to the Faraday cage to allow unobstructed gas flow. A feed gas inlet or an effluent gas outlet are located both above and below the Plexiglas baffles at their respective ends of the reactor. Fittings can be changed to allow the gases to be pumped from below the baffle, above the baffle, or both simultaneously.

Feed gas flow rates are controlled by Whitey needle valves and measured with rotameters calibrated for the gas in use. The pressure inside the reactor is set by adjusting a valve downstream from the reactor outlet. The reactor pressure is monitored by a McLeod gauge with a working range of 0.022–5.0 torr. A liquid-nitrogen cold trap is used to prevent back diffusion of the pump oil into the reactor and to keep fluorocarbons from flowing through the vacuum pump.

An International Plasma Corp. generator with a maximum power of 300 W supplies the radio frequency power at 13.56 MHz. The operating power is measured with a Thruline wattmeter. The reflected power is adjusted to a minimum with a matching LC network.

The electrodes are made of copper sheet metal and are hollow, allowing cooling fluids to circulate within. Both electrodes are cooled during the experiments. To minimize power leakage, the electrically hot electrode is cooled by recirculating mineral oil. The mineral oil is in turn cooled with tap water in a heat exchanger. The ground electrode is cooled with tap water directly. Since cooling the electrodes is more efficient with water than with mineral oil, the surface temperatures of the electrodes are not equal. By alternating the cooling media to the lower electrode where the substrates are placed, the effect of substrate temperature on the rate of plasma polymerization can be ascertained.

The tetrafluoroethylene used in this study was purchased from PCR Research Chemicals and had a purity greater than 97%. Limonene was added by the manufacturer to inhibit thermal polymerization in the tank. GC-mass analysis showed that small amounts of octafluorocyclobutane, a dimer of tetrafluoroethylene, were also present. Helium and argon were supplied by Liquid Carbonic. All gases were used without further purification.

A limited number of infrared spectra of films deposited on KCl crystals were recorded on a Perkin-Elmer 597 infrared spectrometer. Spectra of the virgin KCl crystals were taken first to establish a baseline for comparison with spectra of the films. ESCA spectra were taken on a GCA/McPherson ESCA 36 spectrometer with a MgK_{α} source. Typical operating pressures were on the order of 10^{-7} torr. The electron analyzer has a resolution of 0.02%. All samples were scanned in both the carbon 1s and fluorine 1s region. A deconvolution program was then used to fit the spectra with either Gaussian or Lorentzian peaks. The background and the peak shadows which arise from imperfections in the X-ray monochromatization were subtracted from the data by the program before deconvolution.

RESULTS AND DISCUSSION

Tetrafluoroethylene polymerized either by itself or in the presence of inert gases inside a Faraday cage gave a range of products including oils, films, and powders. The films and oils were either clear or cloudy. The cause of the

cloudiness was suspected to be powder particles trapped in the film or oil formation for the range of experimental conditions investigated. The oils produced in this study were readily soluble in acetone. All film products could be stripped with a tissue soaked in acetone; however, the ease of removal varied from sample to sample. Films scraped from the substrate were only partially soluble in acetone. Diethyl ether also proved to be an effective solvent in stripping the films, but heptane, toluene, methyl alcohol, acetic acid, and water were not.

A polymerization product was also found to cover the entire surface of the upper electrode under all experimental conditions investigated. These films were thicker than those produced in the dark zone and had a brown tint. Some were sticky; others were not. In some instances the films were readily stripped with acetone. The best films were tightly adherent and insoluble in acetone.

The physical properties of the films formed in the dark zone were significantly different from those of conventional plasma-polymerized tetrafluoroethylene and bulk-polymerized polytetrafluorethylene. Conventional plasma polymerization of TFE yields brown films that are somewhat brittle and insoluble in common solvents. Bulk polymerization of tetrafluoroethylene produces a white polymer with strong resistance to chemical attack, insolubility in most solvents, low friction surfaces, and toughness. The films produced in the dark zone were brown, yellow, or off-white. The waxes appeared to have low friction surfaces similar to bulk-polymerized tetrafluoroethylene. Unlike films produced by conventional plasma polymerization of tetrafluoroethylene, the films produced in the dark zone were not brittle. However, they were soluble in acetone to some extent. Bulk-polymerized tetrafluoroethylene is known to be a high molecular weight, crystalline, linear polymer. Conventional plasma polymerization of TFE yields highly crosslinked, amorphous polymers. In contrast, the properties discussed above suggest that the films produced in the dark zone were uncrosslinked, low molecular weight polymers or oligomers.

Infrared spectroscopy did not yield detailed information about the chemical structure of the product; accordingly, only a few of the films produced were analyzed by this technique. Two distinct peaks were present in the spectra. A strong peak ranging from 1400 to 1000 cm^{-1} was attributed to C—F stretching vibration. A second, smaller peak was located at approximately 1725 cm^{-1}. This peak could arise from either C=C or C=O absorption. Absorption due to C=O in hydrocarbon environment normally occurs around 1690–1760 cm^{-1}; however, this peak should be shifted to a higher wavenumber in the presence of fluorine.[22,23] Absorption due to C=C in a hydrocarbon environment often gives peaks around 1626 cm^{-1}. The absorption due to —CF=CF— is reported to be shifted to 1733 cm^{-1},[22,23] lending strong support that the observed second peak is most likely due to C=C absorption in a fluorinated environment.

ECSA proved to be a very useful technique in analyzing the structure of the fluorocarbon polymer products. A major source of information is provided by the chemical shifts within an elemental spectrum. Electronegative elements such as fluorine withdraw electrons from surrounding atoms; thus the effective positive charge felt by core electrons of neighboring nuclei in a fluorinated environment is increased, leading to higher binding energies. This binding energy shift is large enough to be detected by ESCA, yielding important structural information. Hence, the carbon 1s and fluorine 1s ESCA spectra were deconvoluted by Gamet, a computer curve-fitting routine.[24]

Four Gaussian peaks were fitted to the carbon 1s spectrum in Figure 2, a spectrum typical of the more branched polymerization product deposited in the dark zone. These four peaks, in order of decreasing binding energy, have been assigned to carbon bonded to three, two, one, and no fluorines, respectively,[12] labeled as CF_3, CF_2, CF, and C in this paper. Carbon not bonded to fluorine could arise from carbon in highly branched environment or from a hydrocarbon environment that is shifted upfield by beta-fluorines.[11] The latter may be attributed to hydrocarbon contamination incorporated into the fluorocarbon backbone. This factor, however, is expected to be a minor contribution. In scanning the oxygen 1s region, no significant oxygen was observed. For this reason, contributions from carbon bonded to oxygen were assumed to be negligible in the carbon 1s region. What appears to be a fifth peak at 285 eV is actually a peak shadow of one of the upfield peaks. The deconvolution program accounts for these shadows automatically.

Figure 3 shows a typical spectrum of a sample with little if any branching. Here the carbon 1s region is again successfully fitted with four peaks. In Figure 2 all the peaks are of the same order of magnitude, typical of the more branched products, whereas in Figure 3 the CF_2 group is clearly dominant, typical of the more linear products. If CF_3 groups are assumed to be the chain ends, the spectrum in Figure 3 shows that a fairly low molecular weight product was formed. However, satellites of any C=C group may overlap with the CF_3 peak[16,25] and increase its apparent intensity. No estimates of the chain length were made from the ESCA data for this reason.

The ratio of the number of fluorine to carbon atoms (F/C) is another important parameter commonly used to characterize fluorocarbon plasma polymerization products. This parameter can be evaluated by two methods. The first divides the area under the fluorine 1s peak by the total area under the four carbon 1s peaks. This number must then be adjusted by a sensitivity factor which accounts for the different cross sections for photoionization of fluorine and carbon atoms.

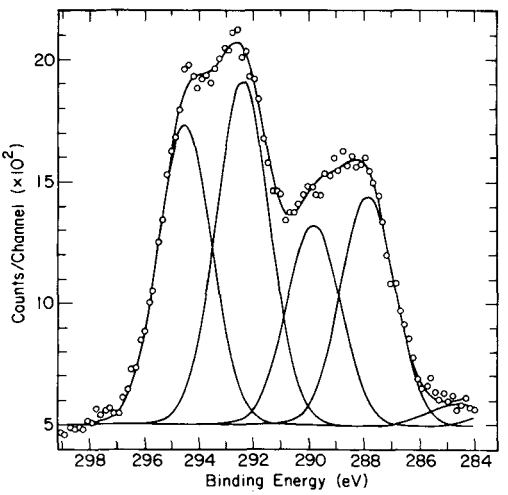

Fig. 2. A carbon 1s ESCA spectrum representative of the more branched polymerization products formed in the dark zone. Circles indicate data points. Smooth curves are fitted by deconvolution program Gamet. He flow rate = TFE flow rate = 10 cc/min (STP); pressure = 0.80 torr; power = 30 W. Substrate placed near the outlet of the reactor.

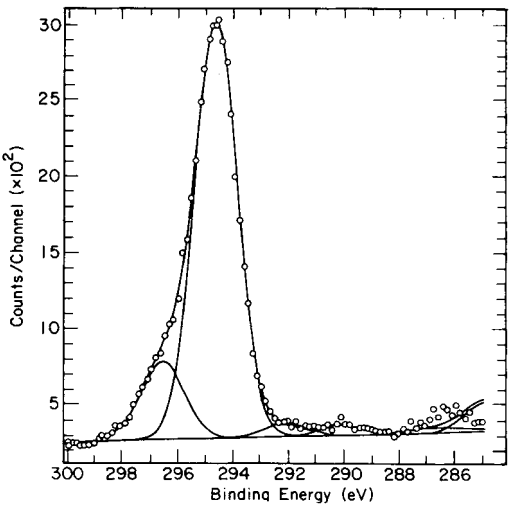

Fig. 3. A carbon 1s ESCA spectrum representative of the more linear polymerization products formed in the dark zone. Circles indicate data points; smooth curves are fitted by deconvolution program Gamet. TFE flow rate = 10 cc/min (STP); pressure = 0.80 torr; power = 30 W. Substrate placed near the inlet of the reactor.

A sensitivity factor of 2.1 was used in the present work.[21] The second method calculates the F/C ratio from the percentage of each group present in the carbon 1s region. This latter method consistently yields a F/C ratio higher by 0.2–0.4 than that calculated by the first method. Such discrepancy has been noted by other authors,[21,26] and it is not yet absolutely clear which method is more accurate. However, the discrepancy is certainly consistent with the aforementioned overlap from a C=C peak in the CF_3 region. In the following discussion the F/C ratio is calculated from the fluorine and carbon peak areas.

Figure 4 shows the percentages of peaks present in the carbon 1s spectra vs. the F/C ratio. Data from different runs correlate well and definite trends emerge.

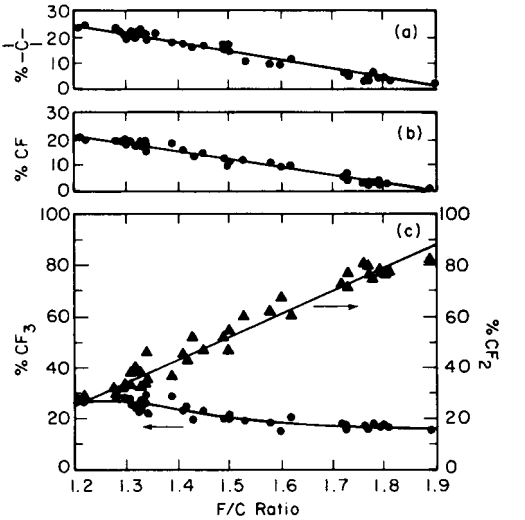

Fig. 4. Percentage of groups present in the carbon 1s spectra vs. the F/C ratio.

As the F/C ratio increases, the percentage of CF and C groups decreases to levels that are difficult to measure accurately with ESCA. The CF_3 group also decreases but levels out at approximately 15% of the total area under the carbon 1s spectrum. The percentage of the CF_2 group increases nearly linearly with the F/C ratio. These results suggest that the number of branch points can be reduced to very low levels, but the number of end groups present in the chain is always quite substantial. Still, sample linearity generally improves as F/C ratio increases.

The full width at half maximum (FWHM) of the peaks in the carbon 1s and the fluorine 1s spectra are plotted vs. the F/C ratio in Figure 5. Again, data from different runs all fall within a certain range and exhibit consistent trends. The FWHM for both elements decreases as the F/C ratio increases. Pender et al.[12] showed that the binding energy of a carbon atom is a function of the elements in the alpha position and, to a lesser extent, of the elements in the beta and higher positions. In a highly branched molecule, the carbon atoms find themselves in a variety of environments, with concomitant broadening of peaks. In a more linear sample, most of the carbon atoms of a group are flanked by CF_2 groups, resulting in narrower peak widths. Figure 5 is consistent with this interpretation.

We now conclude from the above discussion that ESCA is a technique ideally suited for the analysis of fluorocarbon plasma polymers. In the balance of this work, this technique will be used to elucidate the structural dependence on process variables, such as the axial position of the substrate on the bottom electrode, gas flow rate, radio frequency power, substrate temperature, flow pattern and pumping arrangement, and the composition of the feed gas.

A schematic representation of the plasma reactor appears in Figure 6. Solid lines indicate baffles impermeable to gases, whereas dashed lines represent the mesh barrier of the Faraday cage. Gases can cross the screen in either direction. However, the region directly below this barrier is free of electric fields. Inert gases, when used, always entered the reactor through the chamber above the

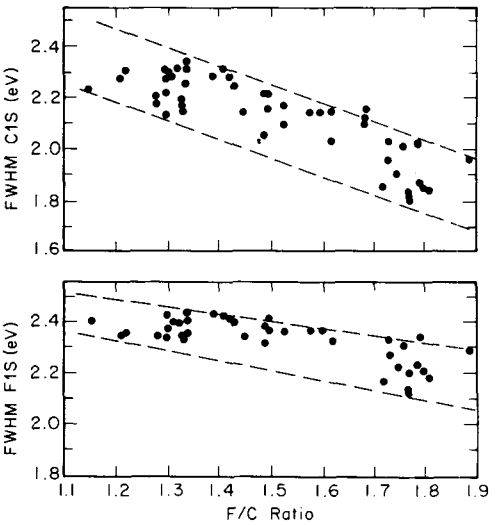

Fig. 5. Full width at half maximum (FWHM) of the peaks in the fluorine 1s and carbon 1s spectra vs. the F/C ratio.

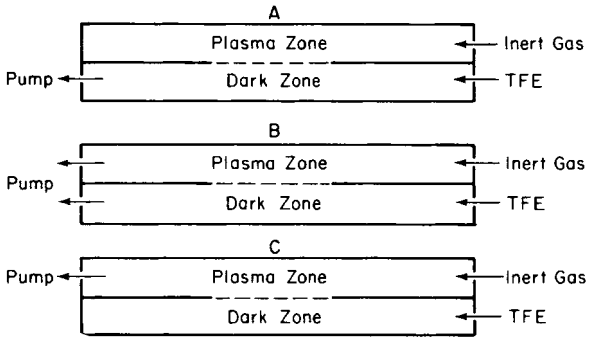

Fig. 6. Schematic representation of the flow arrangement in the plasma reactor. The letters A, B, and C denote the different flow configurations used in the experiments; (—) baffles impermeable to gases; (- - -) mesh barrier of the Faraday cage.

baffle. The entry port for the tetrafluoroethylene was located below the baffle. Effluent gases could be pumped from below the baffle, from above and below the baffle simultaneously, or from above the baffle. These three pumping arrangements are labelled A, B, and C, respectively, in Figure 6. The gases are forced to travel a different path through the reactor in each of these three cases. Unless otherwise stated, arrangement A is implied in the following discussions, since this was the pattern most often used in the experiments.

Flow configuration B was designed to minimize mixing of the feed gases in the reaction zone—the volume between the two electrodes. If only minor mixing of the feed gases occurred in this region, the plasma zone would be filled primarily with inert gas (helium or argon) and the dark zoneBth TFE. Similarly, flow configuration C would increase the concentration of TFE in the plasma zone, and flow configuration A would increase the concentration of inert gas in the dark zone. These three flow configurations would thus be expected to generate significantly different results on the plasma polymerization in the dark zone. The use of two inert gases was motivated by the intrinsic difference in diffusivity, which might lead to different levels of mixing in the reaction zone under the same flow configuration. Results of plasma polymerization using the different gases should therefore reveal the importance of mass transfer.

Figure 7 shows the spatial arrangement of the substrates on the bottom electrode. Unless otherwise stated, the glass slides used to measure deposition rates were placed at the center of the electrode. ESCA substrates were placed at any of the three positions shown, enabling determination of structural changes in

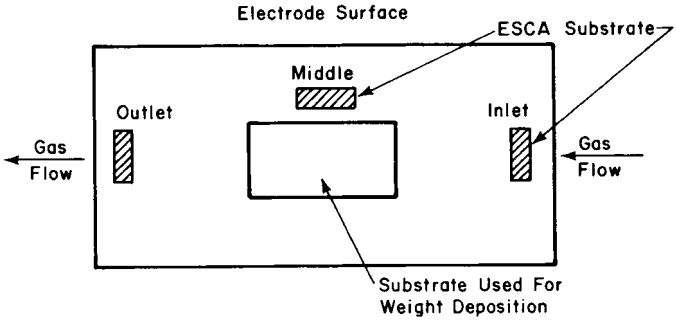

Fig. 7. Schematic diagram of the location of the substrates on the lower electrode.

the product as a function of the axial position on the bottom electrode. These positions are labelled inlet, middle, and outlet in reference to the direction of the gas flow.

In Table I the chemical structures of the polymerization products of a 50% He–50% TFE feed as analyzed by ESCA are listed for all three sample positions and at two power levels. Deposition rates for two experiments are also given. Several important observations can be made here. First, the products are generally more linear near the front of the electrode, i.e., in the upstream direction. This can be attributed to mass transfer and kinetic factors affecting the concentration of free radicals and helium metastables at the electrode surface. In diffusing from the plasma zone to the electrode surface in the field free zone, free radicals and metastables will be swept downstream by the convective flow of gases in the axial direction. Hence, the surface concentration of these species would begin at very low levels at the front of the electrode and build to a plateau further downstream.

The kinetic effect would produce a similar free radical concentration profile at the electrode surface. First assume that, at any point in the plasma, the rate of creation of free radicals is greater than the rate of consumption of free radicals by gas phase recombination, adsorption on solid surfaces, or diffusion from the plasma zone. The concentration of free radicals in the plasma would then increase with axial distance. (Tibbitt et al.[19] predicted such a concentration profile in a butadiene plasma using a free-radical polymerization mechanism.) The rate of diffusion of free radicals to the electrode surface would be roughly proportional to the concentration of free radicals in the plasma above. Ignoring convective mass transfer of free radicals in the axial direction in the dark zone, the concentration profile of free radicals at the electrode surface would then reflect that in the plasma zone, i.e., radical concentration increases with axial distance. Hence, both kinetics and mass transfer affect the concentration profile of free radicals at the electrode surface in the same direction.

If the concentration profile of free radicals and metastables at the electrode surface is indeed as expected, the observation that the products are more linear near the front of the electrode can be readily explained. When present in very low concentrations, most of the free radicals at the electrode surface are consumed in chain initiation. If the concentration of helium metastables is also sufficiently low, a linear product is produced. As the concentration of these species at the electrode surface increases, the creation of branch points along the growing polymer chain becomes significant, resulting in the observed increase of branching with axial distance.

Note that Table I also shows the products to be more branched at higher powers. According to electric discharge theory, an increase in power causes an increase of the electron density in the plasma.[1] This in turn increases the rates of all electron–molecule collision reactions[19] and, consequently, the concentration of free radicals and helium metastables in the plasma. Since the rate of diffusion is concentration-dependent, an increase in the concentration of free radicals and metastables at the electrode surface results at higher powers, creating more branch points in the polymer products. Note also that at high powers the region of the electrode surface where the more branched products are formed increases and extends toward the front edge of the reaction zone. This observation is consistent with the above interpretation, since an increase in power generates

TABLE I
Dependence of Product Chemical Structure on Axial Position for a 50% He–50% TFE Feed[a]

Power (W)	Dep. rate[b] (mg/h·cm²)	CF_3 (%)	CF_2 (%)	CF (%)	C (%)	F/C[c]	F/C[d]	Sample location
10	—	15.7	79.4	2.4	2.5	1.76	2.08	inlet
10	0.025	16.9	77.4	3.2	2.4	1.81	2.09	middle
10	—	21.4	46.3	15.3	17.0	1.50	1.72	outlet
50	—	20.1	52.8	12.3	14.8	1.49	1.78	inlet
50	0.057	23.3	36.8	17.7	22.2	1.33	1.61	middle
50	—	26.4	32.0	19.6	22.0	1.28	1.63	outlet

[a] Deposition condition: He flow rate = TFE flow rate = 10 cc/min (STP); pressure = 0.80 torr.
[b] Deposition rates were measured at the center of the electrode only.
[c] Determined from the ratio of F(1s) and C(1s) spectra.
[d] Determined from the deconvolution of the C(1s) spectrum.

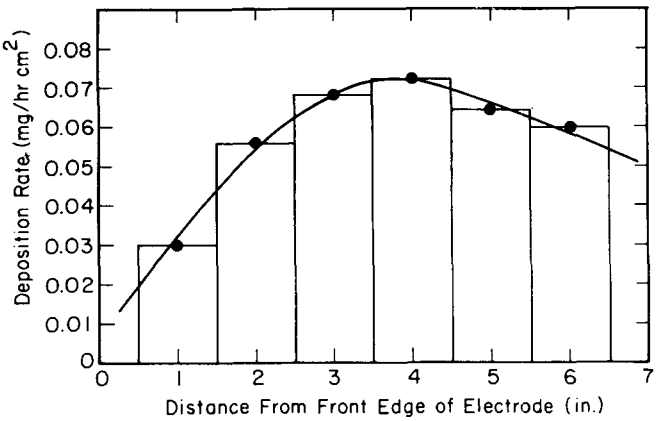

Fig. 8. Deposition rate vs. axial distance. TFE flow rate = 15 cc/min; power = 50 W; pressure = 0.40 Torr.

more free radicals and metastables in the plasma, promoting their diffusion in the substrate surface.

Figure 8 displays the polymer deposition rate as a function of the axial distance for a 100% TFE feed. The reported local deposition rates were averaged over a distance of 1 in., since the glass slides used in the gravimetric measurements were 1 in. wide. The deposition profile is seen to rise rapidly, reach a maximum, and then decline slowly. The initial rapid rise can be attributed to an increase in the concentration of free radicals at the leading edge of the electrode surface. Further increase of the concentrations of free radicals well into the Faraday cage continues to increase the rate of initiation and creates additional branch points for chain growth. Finally the decline in the deposition rate indicates that a point is reached where the concentration of the monomer (TFE) is rate determining, due to the decrease of monomer concentration with axial distance.

Table II lists results from ESCA analyses that correspond to the deposition rates graphed in Figure 8. The product, analyzed only at two of the substrate locations, was linear at the inlet and highly branched at the outlet. These results are similar to the findings for 50% He–50% TFE feeds (Table I) and consistent with the above-mentioned mass transfer and kinetics considerations.

Figure 9 shows the effect of flow rate on the chemical structure and deposition rate. A 50% Ar–50% TFE feed was used in these experiments. Note that the deposition rate decreases slightly over the range of flow rates examined. At the inlet (circles) little if any change in the CF_2/CF_3 ratio was found with the flow rate, the product always being linear. At the outlet (triangles) the CF_2/CF_3 ratio

TABLE II
Dependence of Polymer Structure on Axial Position for a 100% TFE Feed[a]

Sample location	CF_3 (%)	CF_2 (%)	CF (%)	C (%)	F/C[b]	F/C[c]
Inlet	16.4	78.0	2.7	2.9	1.80	2.08
Outlet	27.5	33.9	18.1	20.5	1.42	1.68

[a] Deposition conditions: TFE flow rate = 15 cc/min (STP); power = 50 W; pressure = 0.40 torr.

[b] Determined by F(1s) and C(1s) peak areas.

[c] Determined from deconvolution of C(1s) peak.

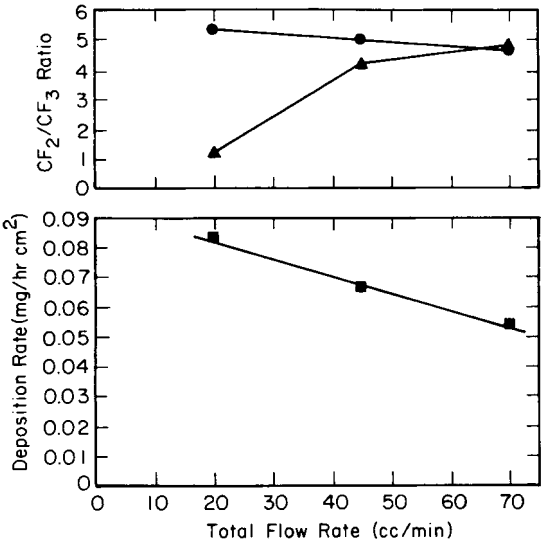

Fig. 9. CF_2/CF_3 ratio and deposition rate vs. total flow rate. Feed composition: 50% Ar–50% TFE; power = 30 W; pressure = 0.60 torr; (●) inlet; (▲) outlet; (■) the center of the electrode.

increased sharply as the flow rate was a little more than doubled; then it increased slowly. Eventually the CF_2/CF_3 ratios at the inlet and outlet become nearly equal at the highest flow rate.

Again these results can be interpreted in the light of either a kinetic or mass transfer effect. The axial velocity of gases in the reaction zone increases as the flow rate is increased at constant pressure. As a result, free radicals and argon metastables are swept away before they diffuse to the lower electrode surface. This leads to an overall lower concentration of these species at the electrode surface. Furthermore, as the axial velocity increases, the residence time of the monomer in the plasma is decreased, causing a decrease in the concentration of free radicals in the plasma and at the electrode surface. A lower concentration of free radicals leads to a more linear product and a lower deposition rate.

The dependence of chemical structure and deposition rate on the substrate temperature is studied next. Results for a 50% Ar–50% TFE feed and a 100% TFE feed are shown in Tables III and IV, respectively. Either water or mineral oil was used to cool the bottom electrode. Cooling with water was more effective than mineral oil and gave lower substrate temperatures. Since these temperatures were not measured during the experiments, they are merely labelled as hot or cold. The data in both tables indicate that the chemical structure of the films is not sensitive to substrate temperature. This was the case at both the inlet and the outlet. Again, for both feeds the product was linear at the inlet and branched at the outlet.

The deposition rate, however, increased significantly at the cold substrate temperature. This was the case for both feeds. The deposition rate is likely enchanced by an increased adsorption of free radicals and monomer at the lower substrate temperatures. Powder formation was noted at the lower substrate temperature for the 100% TFE feed, and could be responsible for the much larger increase in the observed deposition rate.

Figure 10 summarizes the effects of power on the deposition rate and chemical

TABLE III
Dependence of Chemical Structure and Deposition Rate on Substrate Temperature for a 50% Ar–TFE Feed[a]

Dep. rate[b] (mg/h·cm^2)	CF_3 (%)	CF_2 (%)	CF (%)	C (%)	F/C[c]	F/C[d]	Sample location	Substrate temperature
0.196	16.3	78.3	2.3	3.0	1.79	2.08	Inlet	Cold
0.083	15.3	82.0	1.5	1.3	1.89	2.11	Inlet	Hot
—	26.1	29.1	19.9	24.8	1.22	1.56	Outlet	Cold
—	25.7	31.1	19.4	23.8	1.28	1.58	Outlet	Hot

[a] Deposition conditions: Ar flow rate = TFE flow rate = 10 cc/min (STP); power = 30 W; pressure = 0.60 torr.
[b] Deposition rates were measured only at the center of the bottom electrode.
[c] Determined by F(1s) and C(1s) peak areas.
[d] Determined from deconvolution of C(1s) peak.

TABLE IV
Dependence of Chemical Structure and Deposition Rate on Substrate Temperature for a 100% TFE Feed[a]

Dep. rate[b] (mg/h-cm^2)	CF_3 (%)	CF_2 (%)	CF (%)	C (%)	F/C[c]	F/C[d]	Sample location	Substrate temperature
0.347	17.0	75.6	3.4	3.9	1.77	2.06	Inlet	Cold
0.086	17.3	77.1	2.6	3.1	1.80	2.09	Inlet	Hot
—	26.8	28.8	20.5	24.0	1.21	1.58	Outlet	Cold
—	27.4	32.0	19.2	21.4	1.33	1.65	Outlet	Hot

[a] Deposition conditions: TFE flow rate = 10 cc/min (STP); power = 30 W; pressure = 0.40 torr.
[b] Deposition rates were measured at the center of the bottom electrode.
[c] Determined by F(1s) and C(1s) peak areas.
[d] Determined from deconvolution of C(1s) peak.

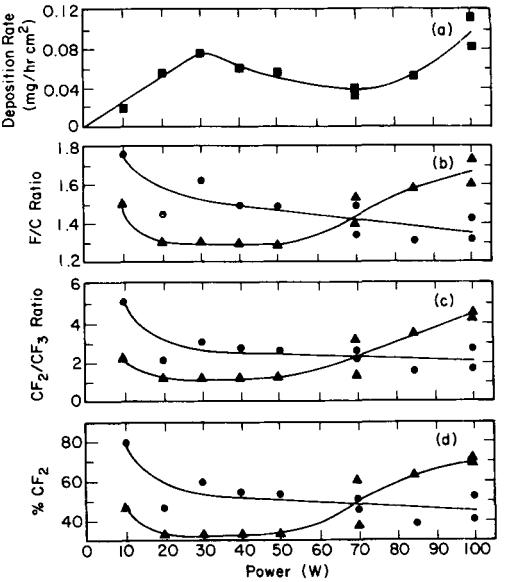

Fig. 10. Dependence of chemical structure and deposition rate on power. Chemical structure is analyzed by ESCA. F/C ratios are calculated from fluorine 1s and carbon and 1s peak areas. He flow rate = TFE flow rate = 10 cc/min. (STP); pressure = 0.80 torr. (■) Deposition rates at the center of the electrode; (●) chemical structure at the inlet; (▲) chemical structure at the outlet.

structure for a 50% He–50% TFE feed. As can be seen from the plot of deposition rate vs. power, the deposition rate initially climbs, decreases slowly, and then increases rapidly at high power. The initial climb in the deposition rate can be attributed to an increase in the concentration of free radicals and helium metastables. The dip in the deposition rate probably results from an increase in the substrate temperature. As the power was increased, a considerable amount of heat was generated within the plasma, causing an appreciable temperature rise at the glass shell of the reactor and at the lower electrode surface at the end of an experiment. The maximum around 30 W indicates that the substrate temperature has risen to a point where adsorption of the monomer and free radicals onto the substrate surface has become rate determining. The increase in the deposition rate at still higher powers is probably due to a significant rate of gas-phase polymerization in the plasma zone. Powdery product from these gas phase reactions can be deposited on the lower electrode, giving rise to the observed increase in the deposition rate. This argument is supported by the observation of powder formation at 100 W.

The behavior of a chemical structure with power was also quite complex. Different trends were observed for the inlet and outlet. At the inlet, the product was linear at the lowest power, 10 W, and rapidly became fairly branched with a small increase in the power. As the power was further increased, a slight increase in the degree of branching was noted. This type of behavior is expected as the concentration of free radicals and mestastables increases. The change in the chemical structure with the power at the outlet is not quite as predictable. Higher powers should yield higher concentrations of free radicals and metastables, and thus highly branched products. This was observed up to 50 W. For powers higher than 70 W, an increase in the linearity of the product deposited

at the outlet position was found. This unexpected result could be a consequence of rapid gas polymerization. In order for this reasoning to be true, it must be assumed that gas phase polymerization yields linear products. Kobayashi et al.[27] investigated the powder formed in an acetylene plasma. Their experiments showed that the powder was a highly crosslinked polymer. Since the powder was not characterized in the present study, no conclusions can be drawn concerning its chemical structure. The above argument thus remains a matter of speculation.

The effect of flow pattern on the chemical structure and deposition rate is given in Table V for a 50% He–50% TFE feed and Table VI for a 50% Ar–50% TFE feed. Very little change occurred in the chemical structure as a result of changing the effluent gas outlet location. For the He–TFE mixed feed, nearly identical chemical structure was found at the outlet substrate position. At the inlet position, a slight increase in the linearity was recorded when the effluent gases were pumped from the lower outlet. The deposition rate was also significantly higher when the effluent gases were pumped from the lower outlet. This result is consistent with a larger number of free radicals and helium metastables being swept to the electrode surface in arrangement A. For the Ar–TFE mixture, however, no effect on the deposition rate or the chemical structure was noticed as the effluent gas outlet was altered.

In Figure 11 the chemical structure of the product and the deposition rate are given as functions of the volume percentage of tetrafluoroethylene in He–TFE feeds at a constant total flow rate. The F/C ratio and the percent of CF_2 peak area in the carbon 1s spectra are the relevant structural parameters here. The ESCA substrates for this set of experiments, as well as the glass slides used for weight deposition measurements, were located at the middle of the lower electrode. Triangles are used to denote data from experiments at a higher substrate temperature (mineral oil cooling), whereas circles represent those at a lower substrate temperature (water cooling). Higher deposition rates were observed at lower substrate temperatures as expected. As the percentage of TFE in the feed is increased, its partial pressure increases also, leading to higher deposition rates.

The product formed in the dark zone was more branched when higher percentages of helium were used in the feed. In order to explain this observation, we need to consider the rates of formation of free radicals and helium metastables as given by the following equations[1,19]:

$$r_{R\cdot} = k_1[M][e] \tag{1}$$

$$r_{He^*} = k_2[He][e] \tag{2}$$

where k_1 and k_2 are rate constants, $[e]$ is the electron density, [M] is the concentration of monomer, and [He] is the concentration of helium. As the percentage of helium in the feed increases, the concentration of helium metastables in the plasma and at the electrode surface should increase, but the corresponding concentration of free radicals is expected to decrease. This, coupled with the above experimental finding, would suggest that helium mestables are more effective than free radicals in creating branch sites in growing polymer chain on the electrode surface. However, the concentration and average energy of the electrons do not necessarily remain constant as the percentage of helium in the feed is altered. Since the kinetic constants k_1 and k_2 depend on the electron

TABLE V
Dependence of Chemical Structure and Deposition Rate on Hydrodynamics for a 50% He–TFE Feed[a]

Dep. rate[b] (mg/h·cm^2)	CF_3 (%)	CF_2 (%)	CF (%)	C (%)	F/C[c]	F/C[d]	Sample location	Flow arrangement
0.076	19.8	59.9	9.3	11.0	1.62	1.89	Inlet	A
0.044	24.3	42.8	15.4	17.5	1.42	1.74	Inlet	B
0.035	22.1	45.4	16.1	16.5	1.41	1.73	Inlet	C
	27.9	32.0	18.7	21.5	1.31	1.66	Outlet	A
	28.8	31.7	19.1	20.4	1.30	1.67	Outlet	B
	28.8	33.4	19.6	18.1	1.34	1.73	Outlet	C

[a] Deposition conditions: He flow rate = TFE flow rate = 10 cc/min (STP); power = 30 W; pressure = 0.80 torr.
[b] Deposition rates were measured at the center of the bottom electrode.
[c] Determined by F(1s) and C(1s) peak areas.
[d] Determined from deconvolution of C(1s) peak.

TABLE VI
Dependence of Chemical Structure and Deposition Rate on Hydrodynamics for a 50% Ar–50% TFE Feed[a]

Dep. rate[b] (mg/h-cm^2)	CF_3 (%)	CF_2 (%)	CF (%)	C (%)	F/C[c]	F/C[d]	Sample location	Flow arrangement
0.083	15.3	82.0	1.5	1.3	1.89	2.11	Inlet	A
0.082	15.6	76.8	3.6	4.0	1.73	2.04	Inlet	B
	25.7	31.1	19.4	23.8	1.28	1.58	Outlet	A
	23.9	29.3	19.8	27.0	1.15	1.50	Outlet	B

[a] Deposition conditions: Ar flow rate = TFE flow rate = 10 cc/min (STP); power = 30 W; pressure = 0.60 torr.
[b] Deposition rates were measured at the center of the electrode.
[c] Determined by F(1s) and C(1s) peak areas.
[d] Determined from deconvolution of C(1s) peak.

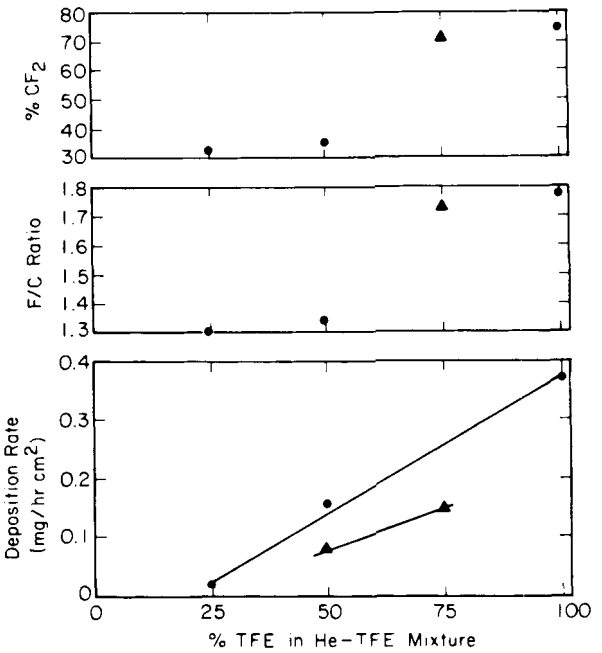

Fig. 11. Dependence of chemical structure and deposition rate on the composition of He–TFE feeds. Total flow rate = 20 cc/min. (STP); power = 30 W; pressure = 0.80 torr. (▲) Higher substrate temperatures; (●) lower substrate temperatures.

energy distribution, the formation of more branched products as the percent of helium in the feed is increased cannot be solely attributed to any specific source but an overall increase in the concentration of reactive species (i.e., free radicals and inert gas metastables combined).

In summary, ESCA was used extensively to study the dependence of product chemical structure on various process parameters of plasma polymerization of TFE, such as flow rate, power, substrate temperature, feed composition, and flow pattern. Information on deposition rates and general physical characteristics were also obtained in this work.

References

1. A. T. Bell, *Techniques and Applications of Plasma Chemistry*, J. R. Hollahan and A. T. Bell, Eds., Wiley, New York, 1974.

2. M. Shen and A. T. Bell, in *ACS Symposium Series 108: Plasma Polymerization*, M. Shen and A. T. Bell, Eds., American Chemical Society, Washington, D.C., 1979, p. 1.

3. J. R. Hollahan, T. Wydeven, and C. Johnson, *Appl. Opt.*, **13**, 1844 (1974).

4. T. Wydeven and R. Kubaki, *Appl. Opt.*, **15**, 132 (1976).

5. D. F. O'Kane and D. W. Rice, *J. Macromol. Sci., Chem. Ed.*, **A10**, 567 (1976).

6. D. Washo, *J. Macromol. Sci., Chem. Ed.*, **A10**, 559 (1976).

7. H. Biederman, S. M. Ojha, and L. Holland, *Thin Solid Films*, **41**, 329 (1977).

8. J. M. Tibbitt, M. Shen, and A. T. Bell, *Thin Solid Films*, **29**, L43 (1975).

9. M. M. Millard and A. E. Pavlath, *J. Macromol. Sci., Chem. Ed.*, **A10**, 579, (1976).

10. A. E. Pavlath and A. G. Pittman, in *ACS Symposium Series 108: Plasma Polymerization*, M. Shen and A. T. Bell, Eds., American Chemical Society, Washington, D.C., 1979, p. 181.

11. A. Dilks and E. Kay, in *ACS Symposium Series 108: Plasma Polymerization*, M. Shen and A. T. Bell, Eds., American Chemical Society, Washington, D.C., 1979, p. 196.

12. M. R. Pender, M. Shen, and A. T. Bell, in *ACS Symposium Series 108: Plasma Polymerization*, American Chemical Society, Washington, D.C., 1979, p. 147.

13. E. Kay, J. W. Coburn, and G. Kruppa, *Le Vide*, **183,** 89 (1976).
14. H. Yasuda and T. Hsu, *J. Polym. Sci.*, **15,** 81 (1977).
15. D. T. Clark, *Adv. Polym. Sci.*, **24,** 126 (1977).
16. D. T. Clark and D. Shuttleworth, *J. Polym. Sci., Polym. Chem. Ed.*, **18,** 27 (1980).
17. K. Nakajima, A. T. Bell, M. Shen, and M. Millard, *J. Appl. Polym. Sci.*, **23,** 2627 (1979).
18. H. Yasuda and T. Hsu, *Surface Sci.*, **76,** 232 (1978).
19. J. M. Tibbitt, R. Jensen, A. T. Bell, and M. Shen, *Macromolecules*, **10,** 647 (1977).
20. H. Yasuda and T. Hsu, *J. Polym. Sci., Polym. Chem. Ed.*, **16,** 415 (1978).
21. A. Salhi, M.S. thesis, Department of Chemical Engineering, University of California, Berkeley, 1980.
22. R. N. Haszeldine, Nature, **168,** 1028 (1951).
23. L. J. Bellamy, *The Infra-red Spectra of Complex Molecules*, Wiley, New York, 1966.
24. C. S. Fadley, Ph.D. thesis, Department of Chemistry, University of California, Berkeley, 1970.
25. D. T. Clark and D. Shuttleworth, *J. Polym. Sci., Polym. Chem. Ed.*, **17,** 1317 (1979).
26. M. Millard, in *Techniques and Applications of Plasma Chemistry*, J. R. Hollahan and A. T. Bell, Eds., Wiley, New York, 1974.
27. H. Kobayashi, Ph.D. thesis, Department of Chemical Engineering, University of California, Berkeley, 1974.

Received January 25, 1982
Accepted April 30, 1982